

**Review of Progress in  
QUANTITATIVE  
NONDESTRUCTIVE  
EVALUATION**

**Edited by Donald O. Thompson  
and Dale E. Chimenti**

**Volume 4B**

Review of Progress in

# QUANTITATIVE NONDESTRUCTIVE EVALUATION

Volume 4B

Edited by

Donald O. Thompson

*Ames Laboratory (USDOE)*

*Iowa State University*

*Ames, Iowa*

and

Dale E. Chimenti

*Materials Laboratory*

*Air Force Wright Aeronautical Laboratories*

*Wright-Patterson Air Force Base*

*Dayton, Ohio*

PLENUM PRESS • NEW YORK AND LONDON

Library of Congress Catalog Card Number 84-646699  
ISBN 0-306-41927-0

Second half of the proceedings of the Eleventh Annual Review of  
Progress in Quantitative Nondestructive Evaluation,  
held July 8-13, 1984, at the University of California,  
San Diego, California

©1985 Plenum Press, New York  
A Division of Plenum Publishing Corporation  
233 Spring Street, New York, N.Y. 10013

All rights reserved

No part of this book may be reproduced, stored in a retrieval system, or transmitted,  
in any form or by any means, electronic, mechanical, photocopying, microfilming,  
recording, or otherwise, without written permission from the Publisher

Printed in the United States of America

## CONTENTS

### VOLUME 4B

#### CHAPTER 4: ACOUSTIC EMISSION, THERMAL AND OPTICAL METHODS

##### Section A: Acoustic Emission

Defect Characterization and Monitoring by Acoustic Emission...	643
C. B. Scruby	
Acoustic Emission Characterization of the Martensitic Phase Transformation in NiTi.....	651
M. Gvishi, M. Rosen and H. N. G. Wadley	
Acoustic Emission Monitoring of Dislocation Motion and Microfracture During Electron Beam Melting and Rapid Solidification of Aluminum Alloys.....	661
Roger B. Clough and Haydn N. G. Wadley	

## CHAPTER 4: (CONTINUED)

Amplification of Acoustic Emission from a Microcrack due to the Presence of a Macrocrack.....	671
J. D. Achenbach	
Acoustic Emissions During Stress Reduction.....	681
G. F. Hawkins, M. Buechler and R. A. Meyer	
Acoustic Emission Monitoring Crack Propagation in Single Crystal Silicon.....	689
C. P. Chen and S-Y. S. Hsu	
Acoustic Emission for On-Line Reactor Monitoring: Results of Intermediate Vessel Test Monitoring and Reactor Hot Functional.....	701
P. H. Hutton and R. J. Kurtz	
An Analysis of Acoustic Emission Detected During Fatigue Testing of an Aircraft.....	709
C. M. Scala, R. A. Coyle and S. J. Bowles	
Interferometric Technique for the Calibration of the Helium Gas Jet Spectrum.....	719
R. R. Sands, W. R. Scott and P. A. Ehrenfeuchter	
Acoustic Emission - Open Discussion.....	727
H. N. G. Wadley, Chairman	
Section B: Thermal Methods	
Thermal Wave Detection of Vertical Cracks in Opaque Solids.....	739
M. J. Lin, L. J. Inglehart, L. D. Favro, P. K. Kuo and R. L. Thomas	
Theory of Mirage Effect Detection of Thermal Waves in Solids.....	745
P. K. Kuo, L. J. Inglehart, E. D. Sandler, M. J. Lin, L. D. Favro and R. L. Thomas	
Resolution Studies for Thermal Wave Imaging.....	753
L. J. Inglehart, D. J. Thomas, M. J. Lin, L. D. Favro, P. K. Kuo and R. L. Thomas	
Phase-Modulated Photoacoustics.....	761
R. G. Stearns, B. T. Khuri-Yakub and G. S. Kino	
Materials Characterization by Thermographic Imaging.....	771
W. Jeffrey Rowe	
Section C: Optical Methods	
Surface Texture Characterization by Angular Distributions of Scattered Light.....	779
Davie E. Gilsinn, Theodore V. Vorburger, Frederic E. Scire, E. Clayton Teague and Michael J. McLay	

## CHAPTER 4: (CONTINUED)

Optical Nondestructive Evaluation of Pipe Inner Wall Condition.....	789
D. L. Cunningham, J. L. Doyle and D. Hoffman	

## Section D: Other Techniques

Locating Surface-Connected Flaws in Ceramics with a Bubble Tester.....	799
William D. Friedman	
Imaging Near Surface Flaws in Ferromagnetic Materials Using Magneto-Optic Detectors.....	807
Gerald L. Fitzpatrick	
Imaging Fatigue with the Gel Electrode.....	819
William J. Baxter	
A Fibre Optic Damage Monitor.....	831
C. K. Jen, G. W. Farnell, M. Parker and P. Cielo	

## CHAPTER 5: MATERIAL PROPERTIES

Needs for Process Control in Advanced Processing of Materials.....	839
Robert Mehrabian and Haydn N. G. Wadley	
Thermal Diffusivity in Pure and Coated Materials.....	859
R. L. Thomas, L. J. Inglehart, M. J. Lin, L. D. Favro and P. K. Kuo	
Nondestructive Determination of Mechanical Properties.....	867
Eckhardt Schneider, Shyr-Liang Chu and Kamel Salama	
Determination of Inhomogeneities of Elastic Modulus and Density Using Acoustic Dimensional Resonance.....	877
L. R. Testardi, S. J. Norton and T. Hsieh	
High Precision Ultrasonic Velocity and Attenuation Measurements of Lamb Waves in Anisotropic Plates.....	881
Robert W. Reed	
Elastic Constants Evaluation Using the Dispersive Property of Acoustic Waves.....	889
C. K. Jen, J. Bussiere, G. W. Farnell, E. L. Adler and M. Esonu	
Elastic Wave Propagation Through Polycrystals.....	901
J. E. Gubernatis and A. A. Maradudin	
Ultrasonic Characterization of Porosity: Theory.....	909
James H. Rose	
Ultrasonic Determination of Porosity in Cast Aluminum.....	919
Shaio-Wen Wang, Antal Csakany, Laszlo Adler and Carroll Mobley	

## CHAPTER 5: (CONTINUED)

Effect of Microstructure and Prior Austenite Grain Size on Acoustic Velocity and Attenuation in Steel.....	927
N. Gryeli and J. C. Shyne	
Ultrasonic Grain Size Evaluation of Heat-Treated Stainless Steel Samples.....	939
Jafar Saniie and Nihat M. Bilgutay	
Non-Destructive Magnetic Method for Detection of the Fatigue and the Dynamic Straining Processes of Ferromagnetic Metals.....	947
Pekka Ruuskanen and Pentti Kettunen	
A Nondestructive Method for Detecting Machining Damage in Beryllium.....	957
R. D. Weglein, J. E. Hanafee and S. E. Benson	
Infrared Detection of Ultrasonic Absorption and Application to the Determination of Absorption in Steel.....	965
Jean-Pierre Monchalin and Jean F. Bussiere	
The Role of the Reflection Coefficient in Precision Measurement of Ultrasonic Attenuation.....	975
Edward R. Generazio	
Reversed Acoustic Attenuation Pattern at the Neck of Tensile Specimen.....	991
G. H. Thomas, S. H. Goods and A. F. Emery	
Characterization Methodology for Film Materials Using Wideband Reflection Acoustic Microscopy.....	997
X. Cheng, C. C. Lee and C. S. Tsai	
A Lamb Wave Prediction of Shear Strength of Spot Welds: On Line and Postservice Evaluation.....	1005
S. I. Rokhlin and L. Adler	
New Methods for the Acoustic Evaluation of Materials with Application to Sorbothane.....	1013
Richard W. Harrison and Walter M. Madigosky	
Ultrasonic Inspection of Alloyed Tungsten Bars.....	1023
Henry Hartmann	
Ultrasonic NDE of Non-Newtonian Fluids for Material Processing.....	1027
B. R. Tittmann, L. A. Ahlberg, J. R. Bulau and F. Cohen-Tenoudji	

## CHAPTER 6: ACOUSTOELASTICITY AND STRESS MEASUREMENTS

Variations in the Acoustoelastic Constants of Aggregates with Finite Grain Size. ....	1035
George C. Johnson and Martin J. Fisher	

## CHAPTER 6: (CONTINUED)

The Acoustoelastic Response of a Rolled Plate: Theoretical Estimate vs. Experiment.....	1043
George C. Johnson	
Acoustoelastic Measurements of Elastic-Plastic and Residual Stresses.....	1051
Martin J. Fisher	
Evaluation of the Absolute Acoustoelastic Stress Measurement Technique.....	1061
S. S. Lee, J. F. Smith and R. B. Thompson	
Acoustoelastic Birefringence in Plastically Deformed Solids.....	1071
Yih-Hsing Pao and Masahiko Hirao	
Nondestructive Detection and Analysis of Stress States with Polarized Ultrasonic Waves.....	1079
Eckhardt Schneider, Holger Pitsch, Sigrun Hirsekorn and Klaus Goebbels	
Experimental Effects of Time-Varying Thermal Gradients on Ultrasonic Waves in Locally Stressed Metals.....	1089
Wallace L. Anderson	
The Use of Off-Axis SH-Waves to Map Out Three Dimensional Stresses in Orthotropic Plates.....	1095
Alfred V. Clark, Jr. and Richard B. Mignogna	
Relationship Between Temperature Dependence of Ultrasonic Velocity and Stress.....	1109
Kamel Salama	
An Ultrasonic Technique for Measuring of Closure Forces.....	1121
Sam Golan	
Effects of Surface Residual Stress on Crack Behavior and Fracture Stress in Ceramics.....	1133
B. T. Khuri-Yakub and L. R. Clarke	
Ferromagnetic Hysteresis and the Effects of Stress on Magnetisation.....	1141
D. C. Jiles	
Stress and Deformation Analysis of a Tube and Coupling Device.....	1151
T. J. Rudolphi and T. R. Rogge	

## CHAPTER 7: ELECTRONIC AND COMPOSITE MATERIALS

## Section A: Electronic Devices

Measurement Techniques for Electronic Devices.....	1159
Gordon S. Kino	



## CHAPTER 7: (CONTINUED)

Thermal Wave Imaging for NDE of Electronic Components.....	1177
R. L. Thomas, Allan Rosencwaig and Jon Opsal	

## Section B: Structural Composites

Assessment of Significance of Defects in Laminated Composites - A Review of the State of the Art.....	1189
S. N. Chatterjee, K. W. Buesking, B. W. Rosen and W. R. Scott	

Ultrasonic Characterization of Changes in Viscoelastic Properties of Epoxy During Cure.....	1203
William P. Winfree and F. Raymond Parker	

Microwave Measurement of the Complex Dielectric Tensor of Anisotropic Slab Materials.....	1209
R. J. King, Y. H. Yen and W. L. James	

Characterization of a Graphite/Epoxy Laminate by Electrical Resistivity Measurements.....	1219
David K. Hsu	

Eddy Current Inspection of Broken Fiber Flaws in Nonmetallic Fiber Composites.....	1229
S. N. Vernon and P. M. Gammell	

Application of Medical Computer Tomography (CT) Scanners to Advanced Aerospace Composites.....	1239
K. D. Friddell, A. R. Lowrey and B. M. Lempriere	

Computer Aided Ultrasonic Flaw Growth Characterization in Composite Structures.....	1247
Robert A. Blake	

Ultrasonic and Thermographic Examination of Composite Tubular Joints.....	1255
Alexander J. Rogovsky	

Prediction of Metal Matrix Composite Density Gradients by Ultrasonic Wave Propagation Velocity Mapping.....	1263
Scott W. Schramm	

Implementation of a Robotic Manipulator for the Ultrasonic Inspection of Composite Structures.....	1269
Robert A. Blake, Jr.	

## CHAPTER 8: PRODUCT LIABILITY AND NDE SYSTEM RELIABILITY

## Section A: Product Liability

The Product Liability Implications of Nondestructive Evaluation.....	1281
O. Smith	

## CHAPTER 8: (CONTINUED)

Products Liability from the Insuror's Standpoint .....	1289
William Lutts	

## Section B: NDE System Reliability

Nondestructive Measurement System Performance: Statistical Characterization.....	1297
K. W. Fertig	

Requirements of Quantitative NDE in Developing Fracture Control Plans.....	1305
Ronald D. Streit	

Inspection Quality Demonstrations.....	1315
Gary J. Dau	

NDE Capability Modeling From Experimental Data.....	1319
Ward D. Rummel	

The Sample Size and Flaw Size Effects in NDI Reliability Experiments.....	1327
A. P. Berens and P. W. Hovey	

Development of a High Reliability Flaw Characterization Module.....	1335
George J. Gruber, Gary J. Hendrix and Theodore A. Mueller	

## CHAPTER 9: EDUCATION FOR NDE ENGINEERS

## Section A: NDE Education

The Need for NDE Education for Engineers.....	1343
Ward D. Rummel	

NDE Education of Engineers: The Next Step.....	1349
J. C. Duke and H. J. Weiss	

ATTENDEES .....	1373
-----------------	------

CONTRIBUTORS .....	1393
--------------------	------

CONTRIBUTORS INDEX.....	1413
-------------------------	------

SUBJECT INDEX.....	1417
--------------------	------

## DEFECT CHARACTERISATION AND MONITORING BY ACOUSTIC EMISSION

C.B. Scruby

Materials Physics & Metallurgy Division  
AERE, Harwell, Didcot, Oxon, U.K.

### INTRODUCTION

In order to be fully effective, any non-destructive evaluation (NDE) technique must be able not only to indicate the presence of defects, but also to locate them within the specimen, assess their significance (including the elimination of spurious indications), and quantify them in terms of size. During the past 20 years, acoustic emission has been applied to a range of NDE problems (Spanner 1981, Stahlkopf & Dau, 1976) with mixed success. Some of the limitations that have been found are intrinsic to the technique, while others are capable of circumvention provided there are further developments in the way acoustic emission is practised.

The acoustic emission technique can only detect a defect source if the defect is growing or changing in such a way that it radiates elastic waves, and if the amplitude of the waves is great enough to exceed a given threshold in the recording system. Since the wave amplitude is broadly speaking proportional to the rate of change of defect size, it follows that its inability to detect slowly growing defects is in part an intrinsic limitation. However the threshold is controlled by ambient noise, and this is often capable of some reduction by the application of good experimental practice.

The elastic wavefield radiated by a growing crack, for instance, contains all the information required to characterise the crack in terms of its position, orientation, size, etc. (Fig. 1). The problem is that this wavefield is only available for an extremely short time, so that very highly developed detection equipment is needed to maximise the information extracted from the emitted waves. In order to locate the source within the specimen an array of transducers is needed. With most commercial equipment, location is restricted to 2-dimensions. However, in a thick-walled structure the depth of the defect through the thickness is also sometimes required, in which case 3-dimensional location methods must be applied. This paper reports some preliminary work using 3-dimensional source location.

An often stated weakness of acoustic emission is the difficulty in assessing the significance of the data, i.e. discriminating between real

(i.e. associated with the accumulation of damage) and spurious events, and quantifying the results in terms of defect size, etc. Spurious emission events can mostly be eliminated by the combination of spatial filtering (i.e. accepting only those events located within a given domain), and external parameters such as the stress applied to the specimen. Positive identification of data as being signals due to crack growth as opposed say to fretting, is not generally practised. While the positive identification of defect growth may never be possible for some applications of the technique, there are other applications where the elastic waves detected at the transducers are sufficiently well defined to distinguish the radiation fields of defects from insignificant events. An example of identifying significant and spurious emission sources is discussed below.

Methods also exist for quantifying the defect growth by analyzing the measured elastic wavefield. This paper will present the application of acoustic source characterisation techniques to the growth of a crack in 7010 aluminium alloy under cyclic fatigue. Finally, the application of this quantitative approach to the NDE of materials and structures will be discussed.

#### EXPERIMENTAL

The results to be presented were obtained during an extensive study of the growth of a fatigue crack in 7010 aluminium alloy. The dimensions of the compact tension specimen (BS 5447, 1975) were  $W = 40\text{mm}$ ,  $B = 40\text{mm}$ ,  $2H = 48\text{mm}$ . The loading was sinusoidal (0.2 Hz) between 12kN and 24kN ( $R = 0.5$ ). For the location study the transducers were located at (25,0,0); (5,0,24), (12,20,0), (12,-20,0), where the origin is at the centre of the notch, and the loading axis is parallel to the z-axis. The transducers thus sample the full 3-dimensional wavefield. For the crack growth characterisation measurements, the transducer positions were (25,0,0), (5,0,24), (17,0-24), (-5,0,-24), (Fig. 2), thus sampling a vertical section of the elastic wavefield.

The transducers used were developed from a design published by Proctor (1982). The area of contact is  $< 1\text{ mm}^2$  giving omnidirectional, broadband response; their frequency response is acceptably flat up to 3 MHz (-6dB) for sources on the transducer axis. The transducers were calibrated against a capacitive transducer. For this study, the recording system comprised four parallel channels, each with amplifiers, band pass filtering and an analogue/digital converter (sampling frequency 20 MHz, record length 102.4  $\mu\text{s}$ ), Fig. 3.

For the location study (Scruby & Baldwin, 1984), data was obtained at different stages of crack growth. During the first monitoring period of 2800 cycles, 18 events were recorded that were believed to be significant in terms of crack growth. This was based on the following criteria: (a) they occurred approximately at maximum load, (b) the arrival times corresponded approximately to the vicinity of the crack front, (c) the first arrivals were well-defined, broadband pulses as expected from defect sources. The location (x,y,z) of the source event was calculated for each set of four arrival times, and the results are shown plotted in (xz) and (xy) projections in Fig. 4(a). It can be seen that a 3-D "image" is formed from the locus of events. The average values of  $x = 3.2\text{mm}$ ,  $z = -0.5\text{mm}$ , are in good agreement with optical measurements of the positions of the ends of the crack ( $x = 2.9\text{mm}$ ,  $z = 0.0\text{mm}$ ) at the end of the monitoring period. It is believed (Weatherly,

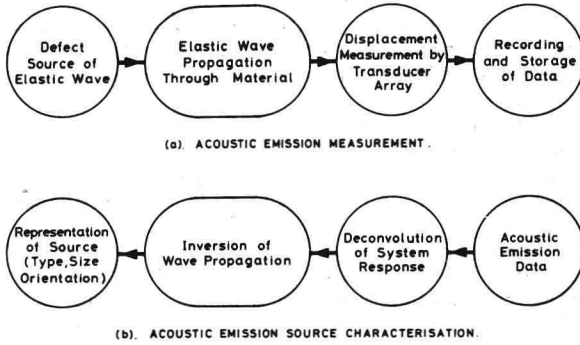


Fig. 1 Acoustic Emission Measurement and Source Characterisation

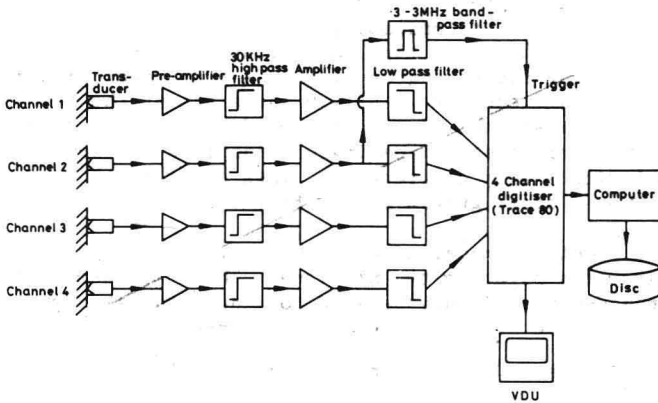


Fig. 2 Compact Tension Specimen used for Characterisation of Fatigue Crack-Growth

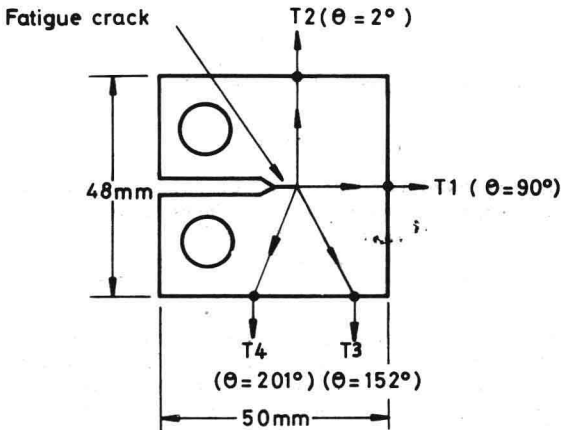


Fig. 3 Multichannel Acoustic Emission Recording System

Titchmarsh and Scruby, 1984) that the primary emission source is inclusion fracture at the crack-tip or within the plastic zone (diameter  $\sim 1\text{mm}$ ), so that Fig. 4 is in fact an image of the crack front.

During another monitoring period,  $\sim 3000$  cycles later, a further 30 significant events were recorded, and these are plotted in Fig. 4(b), where clear evidence of crack advance can be seen. Again there was good agreement with optical measurements of the ends of the crack.

Crack growth characterisation studies (Scruby, Baldwin & Stacey, 1984) were carried out in between the two periods of 3-D source location measurement. During this experiment the transducers sampled a 2-D section of the radiated wavefield, so that information was only obtained about stresses at the source in the (xz) plane. The extension to 3-D is discussed below.

Signals were recorded during  $\sim 1100$  cycles of monitoring. Of these 36 were of sufficient amplitude to measure the direct compression wave arrival strengths on all four channels. The arrival strength was measured as the time integral of each pulse. It was confirmed that the events were recorded close to maximum load, and that the deduced source location was close to the crack tip. A typical signal is shown in Fig. 5. Generally speaking the strengths of  $P_2$ ,  $P_3$  &  $P_4$  were comparable, while  $P_1$  was about half the size. Fig. 6 shows one of the few spurious events recorded. The arrival times correspond to a source close to a loading pin. The arrival strengths include positive and negative values, which indicate slip or fretting. This event is thus readily distinguished from a crack growth event (Fig. 5).

The source event was modelled as a combination of paired forces (dipoles) acting at a point in the xz-plane. The compression arrivals at the four transducers can only be used to deduce the strengths of the dipoles that lie in the xz-plane, so that each source event is written

$$[D_{ij}] = \begin{bmatrix} D_{11} & D_{13} \\ D_{31} & D_{33} \end{bmatrix} \quad \text{where } D_{13} = D_{31} \text{ for no net rotation of the source.}$$

Using the Green's Tensor formulation for wave propagation, the displacements at the transducers are given by

$$U_k = G_{ki,j} D_{ij}$$

Thus the source tensor was deduced by matrix inversion, i.e.

$$D_{ij} = [G_{ki,j}]^{-1} U_k$$

This procedure was followed for each event, using a least-squares procedure to solve the four equations for three unknowns,  $D_{11}, D_{33}, D_{13}$ . The orientation of each source tensor and its principal components were then determined. Each event could then be interpreted in terms of its type, orientation and size. The source type was inferred from the relative strengths of the principal components, which describe the mode of loading (stress field) at the source, or which alternatively can be interpreted in terms of source displacements. In the absence of 3-D information, assumptions had to be made about the measured  $D_{22}$  component. It was decided to characterise the events into four types: dilatation ( $D_{11} = D_{33}$ ), shear ( $D_{11} = -D_{33}$ ), microcrack ( $D_{11} \approx 0.5 D_{33}$ ),

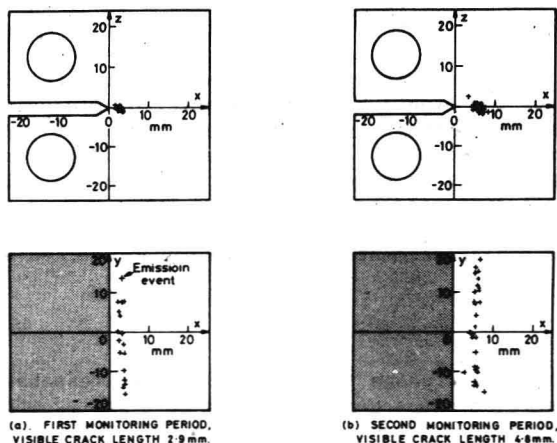


Fig. 4. Position of crack front in xz and xy planes as deduced from location of emission events.

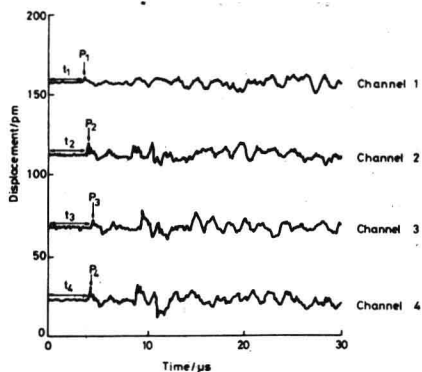


Fig. 5 Typical crack growth event

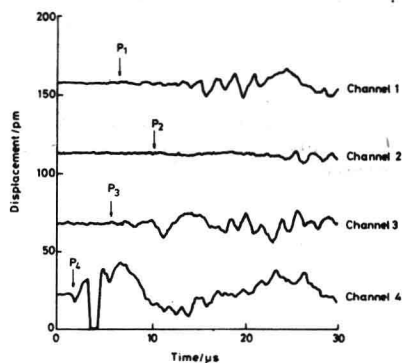


Fig. 6 Spurious event

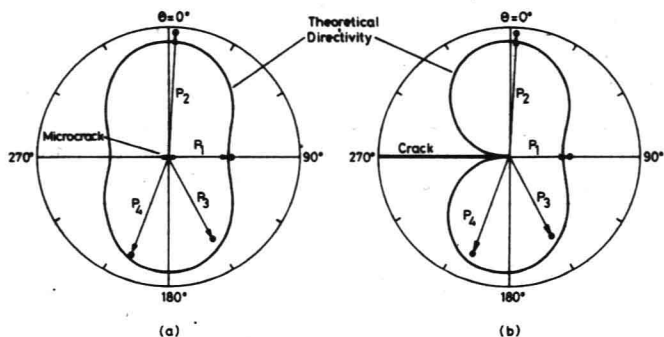


Fig. 7 Experimental data for typical event correlates well with either (a) formation of microcrack, or (b) growth of macrocrack

or single dipole ( $D_{11} = 0$  or  $D_{33} = 0$ ). Table 1 shows the results of applying this characterisation procedure to some test data.

When this procedure was applied to the experimental data, it was found that 80% of the events had the character of microcracks, i.e. they corresponded to the combination of stresses produced by an elastic crack opening under mode I loading. The average orientation was horizontal, and the average strength corresponded to crack opening volume of  $\sim 2000 \mu\text{m}^3$ . Five consecutive results are shown in Table 2. As a check on the inversion procedure, the deduced source parameters were used to calculate surface displacements, which were then checked against the data.

## DISCUSSION

The location study shows that, provided fast response transducers are used, acoustic emission can be applied to crack growth monitoring with a high degree of accuracy (in this case  $\pm 0.5 \text{ mm}$ ). For this material the predominant emission source is almost certainly inclusion fracture, either at, or very close to the crack tip. Provided crack growth, or associated crack tip processes are noisy, 3-dimensional location should be very useful in characterising crack growth in specimens or structures. It is of course necessary to have the transducers close enough to the source to detect the direct wave arrivals. Even secondary sources of emission during fatigue, such as crack face fretting could be used as a means of monitoring crack growth if they occurred near enough to the crack-tip. A particularly fascinating application would be to monitor the shape of a crack front as it advances through a non-uniform microstructure, in for instance a weldment.

TABLE 1  
2-D SOURCE CHARACTERISATION - TEST DATA

SOURCE LOCATION (x, y, z)	P-WAVE ARRIVAL STRENGTHS (pm- $\mu\text{s}$ )				DEDUCED SOURCE CHARACTERISTICS		
	P <sub>1</sub>	P <sub>2</sub>	P <sub>3</sub>	P <sub>4</sub>	TYPE	STRENGTH	ORIENTATION
(4,0,0)	0.8020	0.7005	0.5448	0.6159	Dilatation	1000 $\mu\text{m}^3$	-
(4,0,0)	-0.3007	0.2618	0.1116	0.1740	Shear	1000 $\mu\text{m}^3$	Oblique (45°)
(4,0,0)	0.6015	1.0499	0.7245	0.8669	Micro-crack	1000 $\mu\text{m}^3$	Horizontal (0°)
(4,0,0)	0.9022	0.7662	0.7841	0.5410	Micro-crack	1000 $\mu\text{m}^3$	Oblique (45°)
(4,0,0)	0.0000	0.9366	0.5642	0.7232	Dipole	100 N- $\mu\text{m}$	Vertical 90°



TABLE 2  
2-D SOURCE CHARACTERISATION - FATIGUE DATA

SOURCE LOCATION		P-WAVE ARRIVAL STRENGTHS (pm- $\mu$ s)				DEDUCED SOURCE CHARACTERISTICS		
x	z	P <sub>1</sub>	P <sub>2</sub>	P <sub>3</sub>	P <sub>4</sub>	TYPE	STRENGTH	ORIENTATION
3.5	0.4	0.256	0.624	0.236	0.234	Micro-crack	420 $\mu$ m <sup>3</sup>	Horizontal (2°)
4.1	-0.2	0.631	1.032	0.702	0.917	Micro-crack	1000 $\mu$ m <sup>3</sup>	Horizontal (-7°)
3.9	-0.1	0.388	0.932	0.579	0.681	Micro-crack	840 $\mu$ m <sup>3</sup>	Horizontal (2°)
3.8	-0.3	0.297	0.566	0.383	0.547	Micro-crack	580 $\mu$ m <sup>3</sup>	Horizontal (-9°)
4.1	-0.2	0.642	2.009	1.277	1.672	Micro-crack	1930 $\mu$ m <sup>3</sup>	Horizontal (-3°)

Acoustic emission source characterisation by quantitative measurement and analysis technique should also find applications in the laboratory and field. The present study has shown that the technique is well able to characterise fatigue crack advance under laboratory testing conditions. The 2-D characterisation procedure is executed almost instantaneously (< 1 second per event) using a mini-computer. A comparable 3-D characterisation procedure using 6 transducers takes slightly longer (~ 5 seconds per event). While this method is relatively quick and can be applied in the field, it is liable to inaccuracies, especially in the deduced orientation angles. The alternative approach of deconvolving a substantial portion of the waveform recorded at each transducer, is likely to give superior accuracy, although at the expense of a much longer time for analysis.

There is some evidence in these tests that the pre-crack has "amplified" the size of each source event, as it relaxes and opens under the changing stresses (Wadley & Scruby 1983, Achenbach, Hirashima & Ohno, 1983). The analysis procedure above assumes a point source, although the differences between the compression wavefields of microcrack opening and pre-crack growth (Achenbach & Harris, 1973) are small at the four transducer positions (Fig. 7), and the fit with the experimental data equally good. It is interesting to speculate on the influence of the precrack on a mode II or mode III source at, or near, the crack tip. Further experimental data and theoretical calculations are needed to understand fully how the presence of the macrocrack influences or changes the character of the source at its tip.

It is hoped that these and other source characterisation methods will in the future be applied whenever possible to the monitoring of defects in laboratory specimens and engineering structures. The author has recently been involved with two trial applications of quantitative acoustic emission techniques to industrial pressure vessel testing. Preliminary results have been generally encouraging for quantitative